Fluctuation dynamics of spherical vesicles: Frustration of regular bulk dissipation into subdiffusive relaxation

Laura R. Arriaga,[1] Iván López-Montero,[1] Guillermo Orts-Gil,[2] Bela Farago,[3] Thomas Hellweg,[4,*] and Francisco Monroy[1,†]
[1]*Mechanics of Biological Membranes and Biorheology, Universidad Complutense de Madrid, 28040 Madrid, Spain*
[2]*Stranski-Laboratorium für Physikalische und Theoretische Chemie, TU Berlin, Strasse des 17 Juni 124, 10623 Berlin, Germany*
[3]*Institut Laue Langevin, 6 rue Jules Horowitz, BP 156, F38042 Grenoble Cedex 9, France*
[4]*Physikalische Chemie I, Univeristät Bayreuth, Universitätsstraße 30, 95447 Bayreuth, Germany*
(Received 7 May 2009; published 21 September 2009)

Spherical lipid vesicles obtained by the extrusion method are nonequilibrium membrane structures more curved than the zero spontaneous curvature equilibrium state of the bilayer. Furthermore, these structures are quite rigid as compared to spontaneous vesicles or microemulsion droplets made of soluble surfactants. The dynamical description of the shape fluctuations derived by Milner and Safran (MS) [Phys. Rev. A **36**, 4371 (1987)], which is based on the elastic Helfrich energy referred to the equilibrium state, could be misleading in these cases. In the present contribution, shape fluctuations of unilamellar palmitoyl-oleyl-phosphocholine (POPC) vesicles (radius $R_h \leq 100$ nm) prepared by extrusion are studied by means of neutron spin echo (NSE) in combination with dynamic light scattering (DLS). The relaxation of the fluctuation modes is inferred from the DLS autocorrelation functions and from the intermediate NSE scattering functions measured for several different values of the wave vector. The observed relaxations are compatible with a stretched-exponential decay rather than the single-exponential behavior. Dynamical frustration of the bulk dissipation mechanism in the way described by Zilman and Granek (ZG) for weak amplitude fluctuations [Phys. Rev. Lett. **77**, 4788 (1996)] is invoked as a plausible scenario for explaining the subdiffusive nonexponential relaxations experimentally observed. The combined analysis of NSE and DLS data allows a calculation of the bending elastic constant of POPC vesicles $\kappa = 19 \pm 2\ k_B T$, in excellent agreement with literature data. The ZG approach is revealed as the adequate extension of the MS theory to describe fluctuation dynamics of rigid membranes.

DOI: 10.1103/PhysRevE.80.031908 PACS number(s): 87.16.dj, 87.16.dm, 82.70.Uv

I. INTRODUCTION

Unilamellar vesicles are closed spherical shells usually made of a lipid or surfactant bilayer separating an internal fluid from the external suspending medium. These structures are of great interest since they serve as model systems for biological membranes and they are also useful in the context of drug delivery and targeting. Moreover, vesicles are also used as vectors in transfection. Describing the dynamics for these model systems is crucial to understand biologically relevant processes, such as endocytosis or morphological transformations taking place under flow or upon endogenous deformations along the cell cycle (growing and division). Similarly to microemulsion systems, surface tension is practically zero for vesicles, thus, their mechanical response is governed by the bending elastic free-energy contribution of the undulating interfaces [1]. This concept was successfully introduced by Helfrich to describe the amplitude spectrum of the thermal undulations of microemulsion and vesicle systems and later used for their dynamical description [2]. Particularly, the time dependence of the shape fluctuations for spherically closed fluid membranes has been predicted to be exponentially governed by bulk friction. Schneider, Jenkins and Webb first obtained the relaxation function of the undulating planar membrane from the stationary solutions of the Stokes equations describing the motion of the surrounding incompressible fluids subjected to stick boundary conditions [3,4]. Milner and Safran (MS) extended later that result to the general case of nonzero spontaneous curvature. These theories assume that both the surface of the membrane and the volume enclosed are conserved quantities, thus, membrane compression and bulk osmotic contributions do not play a significant role and only bending elasticity is explicitly accounted for. The structure of the deterministic equations establishes that membrane thermal undulations characterized by a wave vector q relax exponentially, i.e., $S(q,t) \sim \exp(-\Gamma_f t)$, with a finite rate which is ultimately determined by the balance between the bending restoring force and viscous dissipation $\Gamma_f \approx (\kappa/4\eta)\, q^3$ (κ is the bending modulus of the membrane and η is the viscosity of the bulk medium) [2]. This physical picture has been productively exploited to understand the fluctuation dynamics of floppy droplets in microemulsion systems [2,5–7]. Lipid vesicles are however much stiffer structures, thus, thermal fluctuations are weaker and difficult to detect than for microemulsion droplets. Furthermore, droplets of microemulsion phases form spontaneously with a radius compatible with the spontaneous curvature of the adsorbed surfactant, however, lipids have near-zero spontaneous curvature; thus lipid vesicles prepared with a finite radius are nonequilibrium structures with respect to the stable noncurved lamellar phase. Scattering techniques have provided a powerful tool to measure thermal shape fluctuations of the interfacial films in microemulsion systems. Because these techniques probe fluctuations over a number of droplets, they make available ensemble-averaged values of the mechanical parameters. As refers vesicles, most

*Corresponding author. thomas.hellweg@uni-bayreuth.de
†Corresponding author. monroy@quim.ucm.es

experimental studies deal with mechanical deformations of giant unilamellar vesicles followed by optical video microscopy [8]. Micropipette manipulation gives access to the mechanical parameters through the changes in curvature upon vesicle suction inside a micropipette [9]. On the other hand, thermal noise causes giant vesicles to undulate with respect to the spherical shape, thus, fast video microscopy techniques allow for a direct observation of the curvature fluctuations. The amplitude spectrum for these thermal fluctuations has been found in rough agreement with the Helfrich theory [1], though recent high-resolution experiments have revealed the chiefly role of hybrid curvature-compression modes at high curvatures [10]. However, very little is known about the relaxation dynamics of the fluctuation modes. In this context, dilute suspensions of monodisperse unilamellar vesicles, as prepared by the extrusion method, are particularly well suited for probing membrane dynamics of isolated lipid bilayers by scattering methods. The aim of the present contribution is to shed light on the problem of vesicle dynamics in the context of the analysis of quasielastic scattering data. In a previous work [11], the presented approach has been already used omitting most theoretical details. Here, fundamental questions such as the adequacy of the MS theory and their limits of applicability will be addressed in view of experimental scattering data obtained by dynamic light-scattering (DLS) and neutron spin-echo (NSE) experiments performed on diluted suspensions of lipid vesicles obtained by extrusion. To our knowledge, only a very limited number of works directly investigates the thermally excited undulations of lipid vesicles. DLS is mainly used to characterize the vesicles with respect to their size and polydispersity, but no internal motions are resolved [12,13]. Recently, Cantú and co-workers revealed a second fast relaxation contribution to the DLS correlation times superposed to the usual translational component [14,15]. This secondary relaxation has been attributed to global shape deformations of the vesicles and interpreted in terms of the MS model [2]. Applied to vesicles, the MS theory explains the qualitative dependence of the relaxation time on the wave vector q but fails to give realistic values for the bending elastic constant κ, which is expected larger than $10k_BT$ for lipid bilayers [16]. Dynamical anomalies have been also detected in sponge and microemulsion phases exposed to scattering techniques [17–20]. Particularly, at large wave vectors the relaxation function cannot be fitted by a single exponential, rather by a stretched one $S(q,t) \sim \exp(-\Gamma_f t)^{\alpha}$ with an exponent $\alpha \approx 0.7$, and the calculated relaxation rates are found slower with increasing stiffness, which is opposite to the trend expected from the MS theory. In the present work, we present combined scattering data from DLS and NSE performed on dilute suspensions of lipid vesicles showing similar anomalies. The results will be discussed in view of the MS theory at the high stiffness limit represented by lipid bilayers. At this limit ($\kappa \gg k_BT$), a renormalization from the regular MS exponential relaxation to an anomalous nonexponential subdiffusive behavior is expected at high wave vectors, as theoretically described by Zilman and Granek (ZG) [21,22]. Furthermore, extruded vesicles are prepared with a nonequilibrium curvature H_0 $(=1/R_0)$ compatible with its radius R_0, while the spontaneous curvature of the lipid bilayer should be zero, i.e., $H_S=1/R_S=0$. The MS approach describes dynamics for small curvature fluctuations with respect to a reference state with a given spontaneous curvature (finite or zero). Although the MS theory has been productively used in the description of the deformations of microemulsion droplets with an equilibrium finite curvature ($H_S>0$), it has never been applied to scrutinize lipid vesicle systems ($H_S \approx 0$). The paper has been organized as follows. Section II contains the theoretical essentials necessary for understanding vesicle dynamics, i.e., the Helfrich Hamiltonian, the MS theory which implements it in the dynamical equations for the spherical geometry, and the renormalization to the ZG theory for rigid membranes at high wave vectors. Section III describes the materials used and the experimental methods utilized. The experimental DLS and NSE data will be presented in Sec. IV together with their discussion in terms of the theories above. Finally, the main conclusions will be summarized in Sec. V.

II. THEORY

A. Dynamics of spherical membranes: Milner-Safran theory

The bending Helfrich Hamiltonian for the elastic membrane considers the change in mechanical free energy under a small change in curvature with respect to the reference state. In general, within the harmonic approximation, the bending energy of the curved membranes reads as [1,23]

$$\delta F = \frac{1}{2}\kappa(H - H_S)^2, \tag{1}$$

where $\delta H = H - H_S$ is the change in the mean curvature ($H = R_1^{-1} + R_2^{-1}$) defined from the principal curvature radii R_1 and R_2.

Microemulsions and some vesicle systems spontaneously form as quasispherical structures with a radius compatible with the shape of the interfacial amphiphile, which imposes the spontaneous curvature of the interface [24–28]. Naturally curved membranes assemble with a spontaneous curvature H_S that represent the equilibrium minimal free-energy state. Consequently, within the considered harmonic approximation, any change in curvature $\delta H = H - H_S$, with respect to the equilibrium shape H_S causes a quadratic increase in free energy, which is a restoring force to recover the equilibrium shape. As a balance between membrane bending and viscous dissipation with the bulk phase, MS first described the fluctuation dynamics of flexible membranes at the spherical topology [2]. The MS theory stands for spherical microemulsion droplets and vesicles with dimensions compatible with the spontaneous curvature H_S $(\approx 1/R_0)$, so thermal curvature fluctuations can be expressed as local changes in radius $R = R_0\,[1 + \delta(\theta, \phi)]$ with respect to the sphere radius R_0. The small dimensionless fluctuation δ is described as a series of spherical harmonics whose q-dependent amplitudes describe the amplitudes of the fluctuation modes. Each undulation mode is characterized by the integer number l, which determines the periodicity of the oscillations allowed in the sphere; their wave vector $q_l = 2\pi/(2\pi R_0/l) = l/R_0$ (the harmonic integer, $l = 1, 2, 3, \ldots$). By considering bulk hydrodynamics, Milner and Safran resolved the dynamical equations

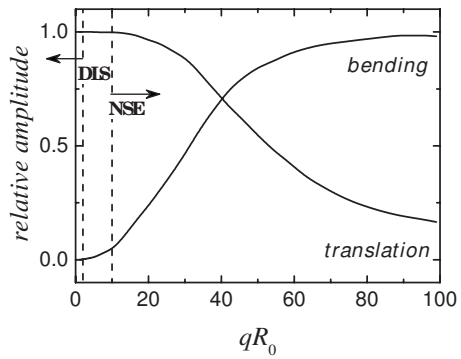

FIG. 1. Normalized amplitudes of the translation (A) and bending ($1-A$) modes as derived from the absolute amplitudes defined in Eq. (A5). The data correspond to the maximal envelope of the oscillatory amplitude functions calculated for lipid vesicles with $R_0=100$ nm and $\kappa=20k_BT$. The MS theory predicts dominant translation and practical absence of bending modes at the DLS window ($q_{DLS}\leq 0.03$ nm^{-1}; $A\approx 1$ and $1-A\approx 0$ at $qR_0\leq 2$). At the NSE window, bending modes start to emerge as a relevant contribution to dynamics. A crossover to a bending dominated regime is expected at $qR_0\approx 40$, well inside the NSE window.

for the fluctuation modes (see details in the Appendix), which are obtained as a sum of discrete spherical modes formally equivalent to the dynamic structure factor obtained for fluctuation modes of long flexible rods [29]. Dissipation within undulation motion is completely dominated by viscous forces and time-dependent amplitudes are found completely overdamped, i.e., $\langle u_l(t)u_l(0)\rangle \sim \exp(\Gamma_l t)$ [see Eq. (A2)]. The dynamic structure factor of the fluctuating shell [see Eq. (A5)] is found as a discrete series of the shape fluctuation modes ($l\geq 2$) subordinated to the pure-translation mode ($l=1$ does not change shape but to a net displacement of the sphere as a whole). Figure 1 shows as the amplitude of the pure-translational term progressively decreases with qR_0 [$A\approx j_0^2\sim (qR_0)^{-2}$], while the sum amplitude corresponding to the undulation modes becomes conversely dominant at high q.

At $qR_0\approx 1$, translation is dominant over fluctuation modes, the only relevant contribution arising from the peanutlike deformation ($l=2$), whose form factor F_l displays its first maximum ($qR_0\approx\pi$) in the vicinity of the first minimum of the translational term [29]. The dynamic structure factor in Eq. (A5) is difficult to unfold; thus it is usually approximated by an "apparent" bimodal function when the $qR_0\approx 1$ regime is scrutinized [6,30–32],

$$S(q,t)\approx e^{-D_T q^2 t}[A+(1-A)e^{-\Gamma_f t}]\approx Ae^{-D_T q^2 t}+(1-A)e^{-\Gamma t}. \tag{2}$$

This is a translation dominated regime ($A\approx 1$; see Fig. 1), where the relaxation rate of the internal "curvature" is controlled by the first fluctuation modes [if the ellipsoidal mode ($l=2$) is the only considered, then $\Gamma\approx\Gamma_{l=2}$]; consequently,

$$\Gamma_f=\Gamma-D_T q^2. \tag{3}$$

If the relaxation function is fitted to a phenomenological effective exponential decay, its "apparent" relaxation rate might be described the initial slope of the dynamic structure factor in Eq. (A5) (equal to the first frequency cumulant); following Ref. [2]:

$$\Gamma(q)\approx \frac{1}{S(q,0)}\left.\frac{\partial S(q,0)}{\partial t}\right|_{t=0} \equiv D_T q^2+\frac{\sum_{l\geq 2}\Gamma_l F_l(qR_0)\langle u_{l0}^2\rangle}{4\pi j_0^2(qR_0)+\sum_{l\geq 2}F_l(qR_0)\langle u_{l0}^2\rangle}. \tag{4}$$

At the opposite limit of high q's ($qR_0\gg 1$), vesicle dynamics is dominated by shape fluctuations and the relative amplitude of the translational mode vanishes (see Fig. 1). At this limit, a continuous description should be possible. In this limit, Eqs. (5)–(7) can be expressed in a continuous form. For lipid bilayers [if $w=0$ and $l\gg 2$ one gets $Z(l)\approx 4/l$], thus, the expressions obtained for planar membranes are recovered [16],

$$\langle u_q^2\rangle\approx\frac{1}{R_0^4}\frac{k_BT}{\kappa q^4}, \tag{5}$$

and

$$\Gamma_f^{(MS)}\approx\frac{\kappa}{4\eta}q^3. \tag{6}$$

These equations show that fluctuation modes have amplitudes decreasing as $\langle u_q^2\rangle\sim q^{-4}$ and relaxation rates increasing as $\Gamma_q\sim q^3$, as described for curvature modes in a planar surface [33]. These equations teach as increasing stiffness does fluctuation modes to relax faster with very small amplitudes. Although the essential physics underlying shape dynamics of spherical shells is well contained in the MS theory, it could still fail in describing such a frustrated relaxation in rigid membranes ($\kappa>10k_BT$), as those made of lipid bilayers.

B. Rigid membranes: Zilman-Granek theory

The q^3 dispersion of the bending modes has been observed for a variety of membrane systems, from sponge phases [19,20] and microemulsion droplets [30–32] to rigid lamellar phases of liquid crystals [31,32,34] phospholipids [8] and polymers [35,36]. However, when probed at high q, the dynamical relaxation of these systems is found anomalous. First, the relaxation decay cannot be fitted by a single exponential rather to a stretched-exponential profile [17,35,36]. Second, the relaxation rate is found decreasing with increasing κ, which is opposite to the trend expected from the dispersion relation in Eqs. (6) and (A3). From the recognition that rigid membranes are not efficient in exploring volume through of bending fluctuations, thus, partially frustrating dissipation against bulk, ZG proposed a plausible explanation for these anomalies. These authors discuss in parallel the anomalous reptation motion of persistent chains and the anomalous relaxation of stiff membranes as two analogous problems [25,37]. These systems consider semiflexible surfaces (one-dimensional chains and two-dimensional membranes) characterized by a persistence length ξ. On length scales shorter than ξ ($q\xi\gg 1$), the object undulates with an elastic bending-energy penalty. On length

scales much larger ($q\xi \ll 1$), however, the object is effectively flexible and its shape can fluctuate with no energy cost. This is the case of flexible chains, which are free to diffuse by reptation in entangled gels. However, for semiflexible objects the reptation diffusion coefficients ($D_{rep} \sim L^{-3}$) and the relaxation times of the fluctuation modes ($\tau_f \sim q^{-3}$) are found with the same scaling than in the classical theories but differ greatly in factors that are dependent on the ratio of the persistence length to the characteristic length of the motion [37]. The ZG theory shows that persistent chains and rigid membranes relax at short length and time scales as a stretched exponential, in contrast with the regular exponential decay describing larger fluctuations in floppy systems [30,31]. By analogy to semiflexible polymer chains, de Gennes and Taupin [25] showed that the floppiness of a two-dimensional membrane is determined by κ with a persistence length ξ,

$$\xi = a \exp\left(\frac{2\pi\kappa}{k_B T}\right), \tag{7}$$

where a represents a molecular length.

If $\kappa \leq k_B T$, thermal fluctuations dominate ($\xi \approx a$), and the vesicle will appear very floppy [38,39]. In contrast, if $\kappa \gg k_B T$, ξ diverges and the vesicle is said to behave rigid. Although the ZG theory was developed for the planar geometry, their main conclusions can be translated to the spherical geometry, thereby, significantly improves the MS theory for the case of rigid membranes. At high q's, curvature changes in rigid membranes are energetically expensive; thus the extensibility of the membrane in the normal direction is dramatically low ($u_z^2 \sim k_B T/\kappa q^4$). The ZG theory explains as bulk viscous friction become frustrated in part within these small-amplitude modes, resulting in an anomalous subdiffusive motion in the transverse direction, which is the natural dynamical consequence of spatially averaging small-amplitude bending modes. The ZG considers a long length scale cutoff ξ determined by the longitudinal size of the membrane. This parameter is identified with the persistence length in Eq. (7) (for rigid vesicles, it is on the order of the vesicle size $\xi \approx R_0$). The limit of the hydrodynamic regime is considered at a short cutoff, the molecular distance a. The ZG theory considers the regular amplitude spectrum and autocorrelation function for the curvature fluctuations, this is

$$\langle u_q(t) u_q(0) \rangle_{reg} \approx \frac{k_B T}{\kappa q^4} \exp(-\Gamma_f^{MS} t), \tag{8}$$

with a relaxation rate given by Eq. (6).

Then, ZG focus on the two-point correlation function $\langle [u(r_1,t) - u(r_2,0)]^2 \rangle$ obtained by continuous integration of the fluctuation modes in the relevant spatial range (ξ, a). This dynamical descriptor is relevant for the calculation of the dynamic structure factor and of the time dependence of the mean-square displacements (MSDs) of the membrane along the transverse direction. This is particularly interesting to identify deviations from the diffusive character of the bending fluctuations (particularly, if $r_1 = r_2$ the two-point autocorrelation function holds for the MSDs at a given point, i.e., $\langle [u(t) - u(0)]^2 \rangle$). It is worthy to notice that the continuous integration performed in the ZG theory is formally equivalent to the mode summation in the MS formalism for the particular case of high curvature fluctuations in a spherical topology [at $q \gg 1/R_0$, summation in Eq. (A5) can be approximated by a continuous integration]. In the ZG theory, the two-point autocorrelation function is separated in two parts: a pure static term $\phi_0(r_1 - r_2)$ plus a dynamic correlator $\phi(r_1 - r_2, t)$. The static correlator ϕ_0 describes the statistically averaged static membrane roughness, and the dynamic one ϕ describes the propagation of the fluctuations with the distance $|r_1 - r_2|$ between two points in the membrane. After some algebra, ZG find

$$\langle [u(r_1,t) - u(r_2,0)]^2 \rangle = \phi_0(r_1 - r_2) + \phi(r_1 - r_2, t), \tag{9}$$

where the static correlator diverges with distance, as expected for bending-energy dominated surfaces; obviating numerical prefactors [22],

$$\phi_0(r_1 - r_2) \sim \frac{k_B T}{4\pi\kappa} |r_1 - r_2|^2. \tag{10}$$

We are mainly concerned by time evolution and dissipation which, following ZG, are governed by the dynamical correlator [22],

$$\phi(r_1 - r_2, t) \approx \frac{1}{\pi}\left[\frac{1}{4}\left(\frac{k_B T}{\kappa}\right)^{1/2} \frac{k_B T}{\eta} t\right]^{2/3} F\left[\frac{|r_1 - r_2|}{d(t)}\right]. \tag{11}$$

Here, the propagator function $F[x(t)]$ is a universal scaling function, which describes the time dependence of the two-point distance $|r_1 - r_2|$ rescaled by the relaxation distance of the bending mode $d(t) = (\kappa t/4\eta)^{1/3}$.

Let us notice that a bending mode with wave vector q relaxes at a rate $\Gamma_f = (\kappa/4\eta) q^3$, thus, the parameter $d(t)$ describes the distance over which the mode extends out during the time t [$\Gamma_f t = (\kappa t/4\eta) q^3 = (qd)^3$]. At short times ($t \ll \Gamma_f^{-1}$), the curvature mode is not yet relaxed covering a distance smaller than its wavelength ($d < q^{-1}$). Conversely, at times longer that the relaxation one, the fluctuation mode covers larger distances (if $\Gamma_f t \gg 1$ then $l \approx q^{-1}$). These dynamical effects result in the above-mentioned frustration. At short times, bending modes do not have time enough to extend out over the whole structure, thus, resulting in a frustrated local relaxation. Contrarily, regular relaxation will be only achieved at long times, where bending modes are able to relax collectively within the MS mechanism. In the ZG theory, the behavior of the nonanalytic propagator function $F[x(t)]$ (the dimensionless distance $x = \delta r/d$) is crucial as it governs the spatiotemporal dependence of the relaxation [21,22,37]. We will be only interested in the two asymptotic limits [see Eq. (12)]. At very small distances with respect to the relaxation one $x(t) \ll 1$, the propagator function reaches a constant asymptotic limit $F[x] \approx 1.34$. On the other hand, at very large distances, $x(t) \gg 1$, it decreases as $F[x] \approx 1/x$. Consequently, two well-differentiated dynamical limits can be observed depending on the length and time scales,

$$\langle [u(r_1,t)-u(r_2,t)]^2\rangle \approx \begin{cases} \dfrac{1}{\pi}\dfrac{1}{|r_1-r_2|}\left(\dfrac{\kappa}{4\eta}\right)t, & at\ \ x(t)\gg 1 \\ \dfrac{3.38}{\pi}\left[\left(\dfrac{k_BT}{\kappa}\right)^{3/2}\left(\dfrac{\kappa}{4\eta}\right)\right]^{2/3}t^{2/3}, & at\ \ x(t)\ll 1. \end{cases} \tag{12}$$

At $x(t)\gg 1$, which actually corresponds to long times ($t \gg \Gamma_f^{-1}$) and large distances ($q \ll d^{-1}$), bending fluctuation modes cause diffusionlike quadratic displacements of the membrane $\langle[\Delta u(t)]^2\rangle \sim D_f t$, with an effective diffusion coefficient inversely proportional to the correlation distance $r_1 - r_2 \sim q^{-1}$, this is $D_f \sim (\kappa/4\eta)q$. Consequently, relaxation is expected in this case to follow a single-exponential profile $\langle u(t)u(0)\rangle \sim \exp(\Gamma_f t)$ characterized by the regular decay rate $\Gamma_f \sim D_f q^2 \sim (\kappa/4\eta)q^3$, i.e., large (high q) bending modes relax regularly with increasing κ, as predicted by the MS theory. Conversely, at short times and small distances [$x(t) \ll 1$], the strong coupling between local and collective motions of the membrane cause bending fluctuations to perform *anomalous subdiffusion* $\langle[\Delta u(t)]^2\rangle \sim t^{2/3}$. This anomalous subdiffusion will subsequently give rise to a stretched-exponential relaxation $\langle u(t)u(0)\rangle \sim \exp(\Gamma_f t)^{2/3}$, as experimentally observed for stiff membranes at high q's. Due to its strongly overdamped character of high curvature deformations in rigid membranes, they are quite inefficient in exploring volume, so dissipation by fluctuations against the bulk is partially frustrated. In this case, one has to wait longer times for relaxation, which is effectively slowed down with respect to smoother fluctuations at low q. The decay rate of the fluctuation modes is found in these cases decreasing with $\kappa^{1/2}$ as [21]

$$\Gamma_f^{(ZG)} \approx 0.025\left(\frac{k_BT}{\kappa}\right)^{1/2}\left(\frac{k_BT}{\eta}\right)q^3. \tag{13}$$

The ZG theory predicts that bending modes in rigid membranes effectively relax at slower rates than regular modes able to explore bulk regions and dissipate energy within. If $\kappa \gg k_BT$ one gets $\Gamma_f^{(ZG)} = 0.1\,(k_BT/\kappa)^{3/2}\Gamma_f^{(MS)}$. This results in a frustration of the regular dissipation mechanism [with single-exponential relaxation $\sim\exp(\Gamma_f t)$] in a subdiffusive relaxation [$\sim\exp(\Gamma_f^{(ZG)}t)^{2/3}$] characterized by a higher effective viscosity than the bulk value $\eta_{eff} \approx 10(\frac{\kappa}{k_BT})^{3/2}$. In these cases ($\kappa \gg k_BT$, $\Gamma_f^{(ZG)} \ll \Gamma_f^{(MS)}$, $ql \gg 1$, and $\Gamma t \ll 1$), the subdiffusive autocorrelation function for the curvature fluctuations is found as follows [21,22]:

$$\langle u_q(t)u_q(0)\rangle_{subdiff} \approx \frac{k_BT}{\kappa q^4}\exp(-\Gamma_f^{(ZG)}t)^{2/3}. \tag{14}$$

Equations (8) and (14) represent the two limit cases of relaxation in elastic membranes, respectively, the regular single-exponential relaxation of floppy membranes at low q and long times, as predicted by the MS theory, and the anomalous stretched-exponential relaxation of small wavelength modes in rigid membranes. The first is typically observed in floppy microemulsion droplets at the $qR_0 \approx 1$ regime [30,31], while the second is characteristic for stiffer membranes in lamellar or vesicle phases. Zilman and Granek argued that both dynamical equations can be unified under a general stretched-exponential profile,

$$\langle u_q(t)u_q(0)\rangle_\alpha \approx \frac{k_BT}{\kappa q^4}\exp(-\Gamma_f t)^\alpha, \tag{15}$$

where the stretching exponent α is

$$\alpha = \frac{2}{3}\left(1+\frac{\nu}{3}\right), \tag{16}$$

with the factor

$$\nu = \frac{3k_BT}{4\pi\kappa}\left[1-0.20\left(\frac{k_BT}{\kappa}\right)^{5/9}\right], \tag{17}$$

and a relaxation rate

$$\Gamma_f = \left[0.025\left(3.69\frac{l(t)}{\xi}\right)^\nu\left(\frac{\kappa}{4\eta}\right)^{\nu/3}\left(\frac{k_BT}{\kappa}\right)^{1/2}\left(\frac{k_BT}{\eta}\right)q^3\right]^{1/(1+\nu/3)}. \tag{18}$$

For $\nu = 3/2$, one gets $\alpha = 1$ and regular exponential relaxation is found. On the other side, $\nu = 0$ holds for stiff membranes ($\kappa \gg k_BT$); then the stretched exponent $\alpha = 2/3$ and the anomalous dispersion $\Gamma_f \sim (k_BT/\kappa)^{1/2}q^3$ are recovered. Note that the dispersion relation $\Gamma_f \sim q^z$ with $z \approx 3/[1 + (k_BT/4\pi\kappa)]$ could exhibit a weak deviation from the regular behavior; however, regular dispersion is expected for membranes stiff enough for ($z \approx 3$ if $\kappa \gg k_BT$).

C. Dynamic structure factor for vesicle systems

At high wave vectors, the dynamic structure factor of a vesicle system is given by the powder average of the single planar membrane structure factor. Within the ZG theory, when this average is performed in the limit of high wave vectors $qR_0 \gg 1$ (the upper limit given by a microscopic length $q \approx a^{-1}$), similarly to Eq. (2), the normalized dynamic structure factor can be written as [21,22]

$$S(q,t) = \exp(-D_T q^2 t)[A + (1-A)\exp(-\Gamma_f t)^\alpha], \tag{19}$$

where the fluctuation term relaxes at a rate given by Eqs. (16)–(18).

The translation amplitude is governed by the *zeroth*-order Bessel function, $A \sim 4\pi j_0^2(qR_0)$. In the high-q regime, where j_0 is practically decayed [at $qR \gg 1$, $j_0(qR) \approx 1/qR$], the translational term should be comparatively small with respect to the fluctuation term (see Fig. 1). On time, diffusional translation is expected to relax much slower than the fluctuation term ($\Gamma_f \gg D_T q^2$). More precisely, the relaxation rates of the bending modes increase as $\Gamma_f \sim q^3$, in contrast with the diffusive translational mode ($\Gamma_T \sim q^2$). Consequently, for rigid vesicles ($\kappa \gg k_BT$), bending modes should be always found relaxing faster than translational ones [$\Gamma_f/\Gamma_T \sim o(\kappa/k_BT)\ qR_0$, thus, at the $qR_0 > 1$ regime $\Gamma_f \gg \Gamma_T$]. Strictly, at $q < (1/D_T t)^{1/2}$, the translational motion is considered essentially nonrelaxed at the experimental window, thus, $\exp(-\Gamma_T t) \approx 1 - o(Dq^2 t)$. Under these conditions, Eq. (19) can be approximated as a linear combination of two

independent relaxation modes. Within this approximation, the dynamic form factor for fluctuating vesicles takes the simpler form,

$$S(q,t) \approx A \exp(-D_T q^2 t) + (1-A)\exp(-\Gamma_f t)^{\alpha}, \quad (20)$$

where the amplitude of the translation mode A and that of the bending mode $1-A$ might be quantitatively similar.

The function in Eq. (20) is the relaxation function ($\alpha = 2/3$) previously used for describing the experimental NSE decays reported for stiff lipid vesicles based on phospholipids and cholesterol [11].

III. MATERIALS AND METHODS

A. Sample preparation

Palmitoyl-oleyl-phosphocholine (POPC) was obtained from Avanti Polar Lipids (Alabaster, AL) at 99% purity. No further purification of this phospholipid was performed. It was stored at −20 °C. These large unilamellar vesicles were prepared by extrusion using a commercial miniextruder. For both experiments (DLS and NSE), solvent was chosen D_2O (sigma; 99.9%, $\eta = 1.2010$ cP at 22 °C). For more details of the procedure, see Ref. [11].

B. DLS: Experimental setup and data analysis

DLS experiments have been performed using a multiangle DLS device (ALV, Langen, Germany) using a diode-pumped Nd-YAG solid-state laser as a monochromatic light source (Compass series, Coherent USA; $\lambda = 532$ nm; output power regulated at 150 mW). The samples were placed in a thermostated bath filled with decaline matching the refractive index of the quartz sample cells. Temperature inside the bath is measured by a Pt-100 sensor and kept constant with a precision of ±0.1°. Measurements were performed at scattering angles ranging from 30° to 120°, at constant temperature (22.0 °C) and vesicle concentration (0.1 mg/mL). The intensity correlation function $g^{(2)}(q,t)$ is measured using a ALV-5000E hardwire correlator. This function is related to the field autocorrelation function $g^{(1)}(q,t)$ through the Siegert's relation,

$$g^{(2)}(q,t) = 1 + C|g^{(1)}(q,t)|^2. \quad (21)$$

The field autocorrelation function is analyzed by CONTIN [40,41], an algorithm based in the inverse Laplace transform. Identical results are obtained by the regularization method (REPES) [42]. No assumption about either the number of relaxation processes or the distribution shape is required in these methods.

C. NSE experiments

The reported NSE experiments were done on the IN15 instrument at the ILL, Grenoble [43]. This instrument provides the longest Fourier times, currently available at NSE instruments. The samples are poured into quartz cells (1 mm thickness; Hellma). The instrument was equipped with a thermostatic holder for these cells and all measurements were done at a temperature of 22 °C. A Fourier time range up to 190 ns was explored at different q values from 0.119 to 1.102 nm^{-1}. To achieve this, measurements at a wavelength of $\lambda = 12$ Å and 15 Å had to be performed. The wavelength distribution in both cases had a full width at half maximum of $\Delta\lambda/\lambda = 0.15$.

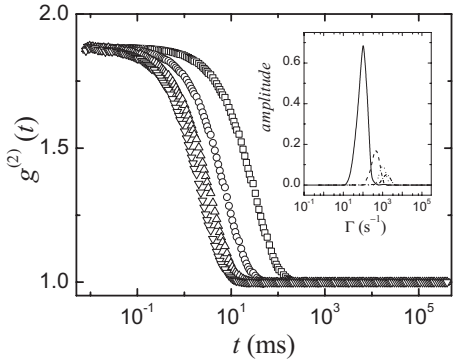

FIG. 2. Experimental DLS autocorrelation functions $g^{(2)}(t)$ for POPC vesicles (extruded through of a 100 nm membrane) at different scattering wave vector; (○) $q = 0.0081$ nm^{-1}; (□) 0.0157 nm^{-1}; (△) 0.0222 nm^{-1}; and (▽) 0.0272 nm^{-1}. Inset: relaxation rate distribution function as calculated by CONTIN.

IV. RESULTS AND DISCUSSION

In this work, we study the fluctuation dynamics of vesicles made of POPC, an unsaturated lipid, which forms well stable vesicles at the fluid phase. The bending elasticity of POPC bilayers has been extensively studied in micropipette experiments performed in giant unilamellar vesicles GUVs [44] and from x-ray experiments on the lamellar phase [45] ($\kappa/k_BT \approx 20 \pm 2$, at room temperature). This assigns POPC membranes a rigid character ($\kappa \gg k_BT$), though relatively flexible as compared to biomimetic lipid mixtures containing cholesterol [16]. Figure 2 shows the scattering intensity autocorrelation functions $g^{(2)}(t)$ obtained from DLS experiments performed on dispersions of POPC vesicles prepared by the extrusion method. Because these dispersions are extremely diluted (1 mg/ml lipid, typically), no interaction effects between vesicles are expected. Indeed, identical results are found independently of the lipid concentration in the range 0.1–2 mg/ml (data not shown). In all cases, CONTIN reveals near exponential relaxation. The distribution of the relaxation times, as calculated by CONTIN, is found indeed rather narrow at low q's ($< 1/R$), as expected for the low size polydispersity intrinsic to the extrusion method (see inset in Fig. 2).

The relaxation-time distribution becomes slightly broader as q increases, which could be attributed either to some size polydispersity arising from smaller vesicles (perhaps lipid aggregates) or to the progressive contribution of undulation modes at $q \geqslant q_2$ ($\approx q_{l=2} = 2/R$). Since shape fluctuations result in an apparent change in the size of the object, both effects are indeed difficult to distinguish. Undulation fluctuations are usually understood to cause additional size polydispersity in floppy droplets in microemulsion systems [32]. Because $g^{(2)}(t)$ are obtained well monodisperse at $q < q_2$, ef-

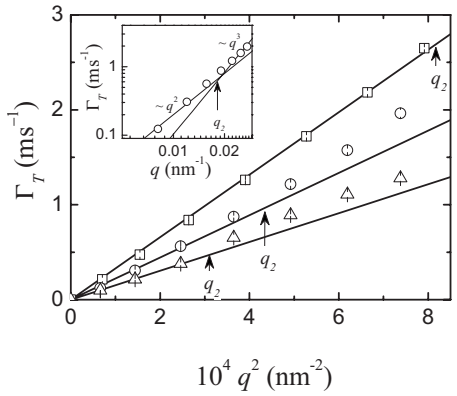

FIG. 3. Relaxation rates of the DLS autocorrelation functions as obtained from CONTIN. The different curves correspond to dispersions of vesicles extruded through membranes with different pore diameter: (□ 80 nm; ○ 100 nm; and △ 200 nm). The straight lines correspond to linear fits to $\Gamma_T = D_0 q^2$. Inset: renormalization from $\sim q^2$ dispersion characteristic of diffusional translation to $\sim q^3$ typical of bendinglike behavior.

fective polydispersity induced by shape fluctuations seems a more plausible scenario for explaining the broader distributions observed at higher q's. Despite of these deviations, center-of-mass diffusional translation is expected to be dominant at the DLS q range (see Fig. 1). The diffusive character of the relaxation rates is verified by the data in Fig. 3, where the relaxation rates obtained by CONTIN are plotted as a function of q^2.

As expected, at low q's ($<q^2$), the experimental relaxation rates are well described by a linear function with a zero intercept ($\Gamma_T = D_T q^2$). Similar behavior is found for every system studied, with the only difference that deviations from the translational diffusive behavior are progressively found at higher q's for smaller vesicles. This is consistent with the idea that fluctuation modes are allowed in a spherical object only with wavelengths shorter than a fundamental oscillation, i.e., $q_l \geq q_2$ ($=2/R$). The relaxation times of the shape fluctuations are, in this regime, probably similar to the diffusional translation times, thus, deconvolution algorithms are unable to discriminate between the modes yielding an average relaxation frequency. Brocca *et al.* [14,15] discriminated both modes by measuring the correlation function extended up to higher q's (at the uv wavelengths), where both motions (translation and bending fluctuations) are expected to relax at a very different timescale. The bare diffusion coefficient for the translation motion can be calculated from the limiting slope corresponding to the low-q data ($\Gamma_T = D_0 q^2$). Vesicle sizes can be then easily calculated from the Stokes-Einstein relation [see Eq. (A7)]; the hydrodynamic radius is obtained as $R_h = k_B T / 6\pi\eta D_0$. To account properly for the translation component, we have performed linear fits to the Γ_T vs q^2 data in the pure-translation regime at $q < q_2$. In practice, this implies fits to five points with just one adjustable parameter. The fitted values of the limiting slope D_0 and the effective low-q value of the hydrodynamic radius are collected in Table I for the samples with a different vesicle size. These results will be later used when analyzing the NSE scattering functions in terms of Eq. (20).

TABLE I. Translational diffusion coefficient D_0 and hydrodynamic radii of POPC large unilamellar vesicle (LUVs) extruded through membranes with different sizes.

Nominal pore diameter (nm)	D_0 10^{12}(m^2/s)	R_h (nm)
80	3.29 ± 0.02	54.7 ± 0.3
100	2.23 ± 0.08	81 ± 2
200	1.52 ± 0.10	118 ± 8

In all cases, vesicle sizes are obtained having radii higher than the nominal radius of the extruder pore size. This effect is caused by two different reasons. The first reason is that due to shear and the floppy character of the vesicles slightly larger sizes are pressed through the pores. The second reason is that DLS does not measure "sizes" but dynamics. Hence, the "size" obtained from DLS actually corresponds to the hydrodynamic radius (vesicles drag the surrounding medium companioned by an external corona of aqueous solvent), thus, R_h values are usually larger compared to the geometrical dimensions [16,46]. However, far from being a difficulty, in measuring relaxation functions from scattering experiments, we are indeed concerned by the translational motion of the "effective hydrodynamic sphere." This might affect the NSE intermediate relaxation as a nontrivial translational contribution at long times.

The observed deviations from the limiting-q^2 pure-translation behavior of the relaxation rates are systematically found at $q > q_2$ with a q^3 dependence. This effect is clearly visible in the log-log plot (see the inset in Fig. 3), where a renormalization from the $\sim q^2$ behavior to a $\sim q^3$ dependence, characteristic for the relaxation of the bending fluctuations is observed at $q > q_2$. Therefore, these deviations can be *a priori* assigned to shape fluctuation modes, which come into play in the DLS time window at $q \geq q_2$. As a first attempt, we discuss the data of Fig. 3 (vesicles, 81 nm radius) in view of the MS theory. The DLS-relaxation rates obtained from CONTIN plotted in Fig. 3 represent an effective rate corresponding to a single-exponential relaxation model for the autocorrelation functions $g^{(2)}(t) \approx e^{-\Gamma t}$; thus they can be assigned to a first cumulant rate.

Figure 4(a) shows predictions from the MS theory for this first cumulant relaxation rate [see Eq. (4)]. These data represent the effect of increasing κ on the relaxation rates. The observed deviations from the pure-translation behavior are consistent with the presence of fluctuation modes, but the observed rates are compatible with abnormally low values of the bending modulus ($\kappa \approx 0.01\ k_B T$; this value would indicate an extremely floppy structure. For microemulsion droplets, one would expect about $1\ k_B T$, but the value found is absolutely unphysical for lipid bilayers.). Reasonable values of κ ($\approx 20\ k_B T$) give rise to much faster rates in view of the MS theory. Although Eq. (4) has been found to successfully describe the relaxation rates of floppy droplets of microemulsion phases ($\kappa \approx k_B T$), the present anomaly has been also observed for a variety of rigid systems ($\kappa > k_B T$) [47,48].

To get insight on the nature of the present anomaly, we have tried to explore the effect of the curvature parameter w

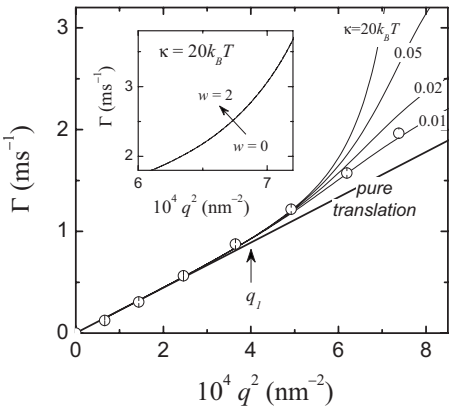

FIG. 4. First cumulant experimental relaxation rates as calculated by CONTIN from the DLS autocorrelation functions obtained for a diluted dispersion of POPC vesicles (81 nm radius). The q^2-translation component is represented by the thick line ($\Gamma_T = D_0 q^2$, with $D_0 = 2.23 \times 10^{-12}$ m^2/s; see Table I). Predictions from the MS theory [Eq. (4)] are represented by thin lines labeled with the different values of the bending stiffness κ. These rates account for the dynamical contribution from every fluctuation mode [the series in Eq. (4) actually extends from the fundamental fluctuation mode (ellipsoidal mode; $l=2$) up to the high-q regime, where mode amplitudes are negligible; in practice, the series is numerically truncated at $l=1000$]. The arrow at $q_1 = 0.02$ nm^{-1} marks the wave vector above which bending modes starts to be allowed in a circular topology ($q_1 = 1/R$), coinciding with the crossover between the pure-translation and mixed regimes, where fluctuation modes start to contribute on dynamics. Inset: dependence of the relaxation rates on the curvature parameter w (for a rigid membrane with $\kappa = 20 k_B T$). No differences are observed in modulating w in the range 0–2.

on the relaxation rates. They have been computed for different values of w (see the inset in Fig. 4), obtaining extremely small differences (not visible in the plot) in the range $w=0$ (zero spontaneous curvature, which is mathematically equivalent to a forcedly curved vesicle $R \ll R_S$) to $w=2$ (nonzero spontaneous curvature, equivalent to a vesicle less curved than at equilibrium, i.e., $R > R_S$). The reported anomaly could arise from the inadequacy of the MS formalism for describing nonequilibrium vesicle states far from the spontaneous curvature ($H = 1/R_0 \gg H_S \approx 0$). As stated above, lipid vesicles are out-of-equilibrium structures, thus they are actually prepared with a higher curvature than the equilibrium value (for the thermodynamically stable lamellar phase, $H_S = 0$). Consequently, the observed fluctuations actually correspond to curvature deviations with respect to a forced nonequilibrium state, so probably the elastic harmonic approximation in Eq. (1) is not adequate so far. Anyway, nonequilibrium vesicles can be considered "kinetically frozen" at their extruded size (at least during a few days); thus, nonequilibrium contributions to the elastic free-energy functional can be, in practice, considered time independent, do not strongly contribute to fluctuation dynamics. Although this point might be theoretically addressed, the weak dynamical influence of the curvature parameter w shown in Fig. 4 (inset) suggests that the above-mentioned off-equilibrium curvature effects are not dominant with respect to the dynamical anomalies observed.

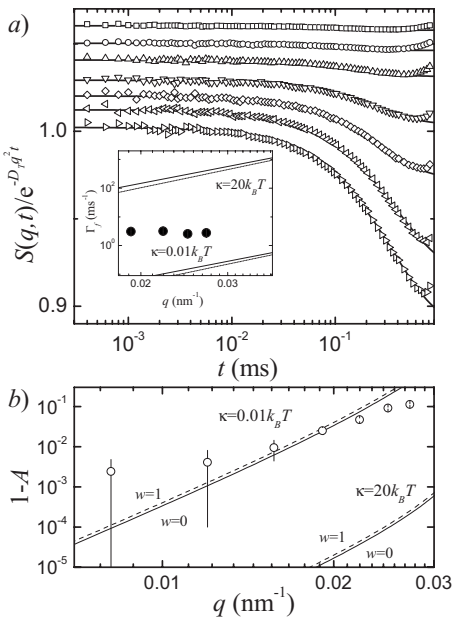

FIG. 5. (a) Relaxation contribution from internal modes to the DLS autocorrelation functions at different q (from top to bottom: 0.0081, 0.0120, 0.0157, 0.0191, 0.0222, 0.0249, and 0.0272 nm^{-1}). For clarity, data at different q have been vertically shifted by an arbitrary amount. Solid lines represent best fits to an exponential model $S_f(q,t) \approx A + (1-A)\exp(-\Gamma_f t)$, as expected from the MS theory [see Eq. (2)]. Inset: (symbols) relaxation rates as obtained from fits. (Lines) predictions from the MS theory [Eq. (A3)]. Down lines: floppy case; $\kappa = 0.01 k_B T$; upper lines: rigid case; $\kappa = 20 k_B T$. Calculations were performed at zero spontaneous curvature ($w=0$; solid lines) and at a curvature equal to the spontaneous radius ($w=1$; dashed lines). (b) Experimental values of the relative amplitudes of the internal relaxation in (a) assigned to bending modes. Lines represent predictions from the MS theory [as computed from Eq. (A5)].

To better analyze the character of these anomalies, we have tried to resolve in the DLS autocorrelation functions the relaxation arising from the fluctuation modes. Fluctuations are isolated by dividing the experimental autocorrelation functions by the pure-translation component, i.e., $S_f(t) \approx g^{(2)}(t)/\exp(-D_0 q^2 t)$ [see Eq. (2)] with D_0 taken from Table I.

At low q's ($<q_2$), extraction of the translational component results in a constant function taking values close to unity within the experimental uncertainty. However, a significant relaxation component with increasing amplitude starts to emerge at $q \geq q_2$, as expected for shape fluctuation modes. Anyway, the observed relaxation is marginal ($\leq 10\%$) with respect to the main translational component, as expected in this regime ($qR \approx 1$; see Fig. 1). The relaxation times calculated from fittings to the usual exponential model $S_f(q,t) \approx A + (1-A)\exp(-\Gamma_f t)$ [see Eq. (2)] do not show a clear dependence on the wave vector. Again, the absolute values of Γ_f are consistent with, unphysical very low values of κ ($<k_B T$) (see the inset in Fig. 5). Bending modes relaxing in the regular sense described by MS might, however, do at a much faster rate than experimentally observed (see data at $\kappa = 20 k_B T$ in the inset in Fig. 5). Further, Fig. 5(b) shows

the relative amplitude of the relaxation component which, although following the expected q increase, is obtained two orders of magnitude higher than quantitative predictions from the MS theory. This behavior assigns the translation mode chiefly dominant at this wave-vector regime ($A \approx 1$ at $qR \approx 1$; see Fig. 1). All these results point to the inadequacy of the MS in quantitatively describing the relaxation of the internal mode observed together with the dominant translational mode. In general, for $\kappa \approx 20 k_B T$ (value typically found for lipid bilayers), the MS predicts bending modes with a much lower amplitude and relaxing much faster than experimentally observed.

Lipid vesicles represent indeed the case of rigid membranes, where the frustration mechanism described by ZG could eventually dominate dynamics of shape fluctuations. Within the frame of ZG theory, if a value $\kappa \approx 20 k_B T$ is assumed, the relaxation distance of the bending modes at the time scale where shape fluctuations are observed (in the DLS window, $t < 0.3$ ms) is estimated to be $d \approx (\kappa t / 4\eta)^{1/3} \leq 140$ nm, which is a distance of the order, but a little bit larger than the spatial scale probed by DLS; since we observe fluctuations modes at $q_{DLS} \geq 1/R \geq 0.02$ nm^{-1}, the dimensionless relaxation parameter $x_{DLS} \approx 1/qd \leq 0.3$. Consequently, one expects the regular relaxation of the bending modes to become frustrated in the way predicted by the ZG theory [see Eq. (20)]. We will turn to this point later. Further insight can be gained in analyzing the NSE intermediate relaxation functions, which explore dynamics at much higher q's than DLS ($q_{NSE} > 0.1$ nm^{-1}). At this regime ($t < 200$ ns, $q > 0.1$ nm^{-1}), the relaxation distance $d \approx (\kappa t / 4\eta)^{1/3} \approx 12$ nm; thus the relaxation mechanism of the bending modes is expected to be subdiffusive also at the q regime probed by NSE ($x_{NSE} \approx 1/qd \leq 0.8$). Consequently, in the studied regimes (both in DLS and NSE), the ZG theory predicts for the present bilayer vesicles a frustration of the regular dissipation mechanism controlled by bulk friction into a subdiffusive relaxation mechanism governed by the stretching exponent α [see Eqs. (15) and (16)]. If $\kappa \approx 20 k_B T$, $\nu \approx 0.011$, thus $\alpha \approx 2/3$, and the κ-dependent effective viscosity $\eta_{eff} \approx 10(\kappa / k_B T)^{3/2}\ \eta \approx 74\ \eta$. For vesicles sized approximately 100 nm radius ($qR \gg 1$), NSE might be able to discriminate translation and bending modes (see Fig. 1). For the sake of example, Fig. 6 shows two intermediate NSE relaxation functions $S(q,t)$ obtained at different scattering wave vectors for a suspension of POPC vesicles ($R_h = 81 \pm 2$ nm) in the range $q_{NSE} = 0.1 - 0.4$ nm^{-1}. In this domain, membrane shape fluctuations might be clearly observable in NSE experiments (q_{NSE}: $10^8 - 10^9$ m^{-1}, for the studied vesicles $qR > 10$).

These relaxation curves might correspond to high-order membrane fluctuations shorter than the vesicle perimeter but large enough as compared to molecular dimensions, i.e., we are probing the spatial regime, $R^{-1} \ll q < a^{-1}$. The considered motion occurring at times shorter than 200 ns must correspond to higher fluctuation harmonics ($q = l/R$) ranging from $l \sim 5$ up to $l \sim 50$. In this regime, bending modes are expected to belong to a time scale well shorter than the translational terminal contribution relaxing at longer times, probably far away from the experimental NSE window. Under these conditions, center-of-mass translation can be considered essentially nonrelaxed; even at the higher q's the translational relaxation time $\tau_T \sim \Gamma_T^{-1}$ $(=1/D_T q^2) \sim 50$ μs is already quite longer than the NSE experimental time ($t_{NSE} \leq 190$ ns). In other words, the considered vesicle shape fluctuations ($l > 5$) occur at a time scale such that the vesicle does not translate so far. These features have been made visible in Fig. 6. At the lowest wave vector probed by NSE ($q = 0.119$ nm^{-1}), the translational relaxation time $\tau_T \sim \Gamma_T^{-1}$ $(=1/D_T q^2) \sim 32$ μs is much longer than the probed time scale; thus the translational component to the relaxation function remains essentially nonrelaxed, i.e., $\exp(-\Gamma_T t) \approx 1$. On the other hand, regular bending modes (in the MS sense) are expected to relax much faster [MS exponential decays in Fig. 6 with $\Gamma_f^{(MS)} = (\kappa/4\eta) q^3$ and $\kappa = 20 k_B T$] at the probed window. Because this function is already completely decayed, it does not contribute to the observed relaxation at all. The observed decrease of $S(q,t)$ in Fig. 6 is definitively due to a relaxation component occurring at the probed time scale. We have plotted the nonexponential relaxation expected for dissipative bending modes as predicted from the ZG theory [$\kappa = 20 k_B T$, $\alpha = 2/3$, $S_f \sim \exp(-\Gamma_f t)^{2/3}$ with $\Gamma_f^{(ZG)} \approx (1/74)(\kappa/4\eta) q^3$]. It is evident that the observed relaxation is only compatible with bending modes as described by ZG theory; otherwise, regular relaxation might take place at a much faster rate, $\Gamma_f^{(MS)} \geq 74\ \Gamma_f^{(ZG)}$. Shape deformation modes are therefore concomitant of vesicle translation at the NSE window. Contrarily to DLS data, fluctuation modes might be the main scattering contribution at the NSE relaxation function (see Fig. 1) though translation might be considered as a terminal contribution leading to its nonzero base line. Consequently, Eq. (19) can be used to interpret the experimental data in Fig. 6. Assuming the validity of the ZG approach in describing the local undulation dynamics of the bilayer of lipid vesicles, $g_{bend}(t) \sim \exp(-\Gamma_{ZG} t)^{2/3}$, Eq. (19) turns on $S(q,t)/S(q,0) = \exp(-\Gamma_T t)$ $[A + (1-A)\exp(-\Gamma_{ZG} t)^{2/3}]$. This expression, similarly to previous approaches unfolding dynamics in microemulsion systems [30–32], might provide an

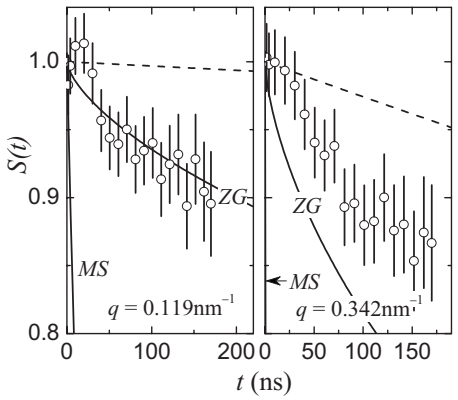

FIG. 6. Nontranslational relaxation effects in the experimental NSE intermediate relaxation functions. Data correspond to POPC vesicles (81 nm radius) at two different wave vectors. Lines correspond to pure modes (i) translational (dashed) and (ii) bending (solid). The bending mode of the rigid membrane ($\kappa = 20 k_B T$) has been chosen to relax: (MS) single exponential with relaxation rate given by Eq. (6); (ZG) stretched exponential ($\alpha = 2/3$) with relaxation rate given by Eq. (13).

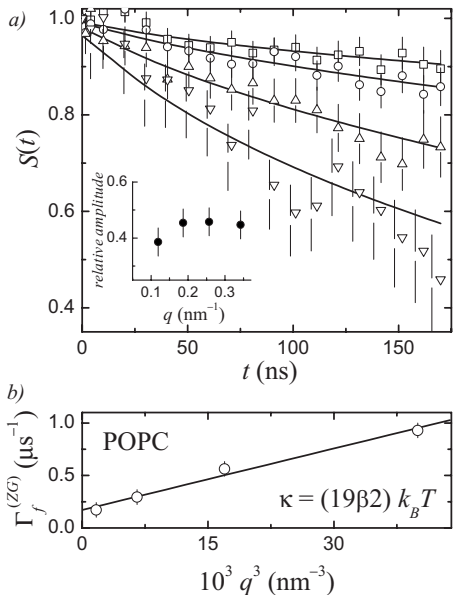

FIG. 7. (a) Experimental NSE intermediate relaxation functions for POPC vesicles (81 nm radius) at different wave vectors. Lines correspond to fits to the ZG approximated Eq. (20) with fixed parameters $\alpha=2/3$ and $D_0=2.23\times10^{-12}$ m^2/s. Inset: relative amplitude of the bending mode $(1-A)$ as obtained from the fits. (b) ZG plot: q^3 dependence of the bending relaxation frequencies as obtained from fittings to the ZG relaxation [Eq. (20)]. Line is the best linear fit, from which a value $k=(19\pm2)$ k_BT of the bending stiffness has been deduced for POPC membranes.

adequate model for describing the NSE scattering functions in vesicle systems. However, no stable fits are achieved in the present case when the three adjustable parameters (A, Γ_T, and Γ_{ZG}) are left to vary. Two *a priori* conditions must be imposed in order to get nonbiased fits: (a) the translational relaxation rate is fixed at the value deduced from the DLS data, i.e., $\Gamma_T(q)=D_0q^2$, and (b) the translational motion is considered essentially nonrelaxed at the NSE window, i.e., $\exp(-D_0q^2t)\approx1-o(D_0q^2t)$. This last is strictly true only at $q\ll(1/Dt_{NSE})^{1/2}$. Under these conditions, the approximated bimodal expression in Eq. (20), which considers both modes (translation and shape fluctuation) relaxing independently, can be reasonably used, $A(q,t)\approx A\exp(-D_0q^2t)+(1-A)\exp(-\Gamma_{ZG}t)^{2/3}$. This approximated expression has been successfully used for fitting our experimental NSE relaxation curves. Predictions from the exact relaxation curve in Eq. (19) differ by less of a 1%, well below the experimental uncertainty (3% typically). In practice, the use of Eq. (20) has been restricted at $q\leq0.4$ nm^{-1} for fitting purposes. Since NSE probes times $t_{NSE}\approx170$ ns, the approximated function in Eq. (20) is reasonably close to the exact expression in the considered q range [for the vesicles considered, 81 nm radius, $D_0\approx10^{-12}$ m^2/s, one gets $(1/Dt_{NSE})^{1/2}\approx2$ nm^{-1}]. This approximated expression describes, in general, a bimodal relaxation, where both modes are dynamically uncoupled. Although, fluctuation modes are internal modes subsidiary of translation of the vesicle as a whole, they can be considered dynamically uncoupled at the considered time scale. Figure 7(a) shows the NSE relaxation functions for POPC vesicles measured at the q range, where Eq.

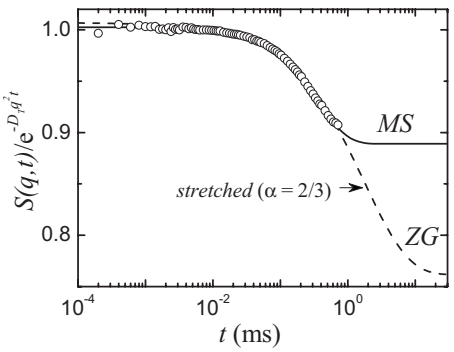

FIG. 8. Reanalysis in terms of the ZG theory of the internal relaxation detected in the DLS autocorrelation functions. Symbols correspond to the experimental data in Fig. 5 ($q=0.027$ nm^{-1}). Lines are the best fits to (MS) a single-exponential decay; (ZG) a stretched exponential with $\alpha=2/3$.

(20) can be considered a good approximation.

The lines in Fig. 7(a) represent the best fits of Eq. (20) to the experimental data, the fitting parameters being the amplitude A, and the relaxation frequency Γ_{ZG} of the fluctuation modes. The translational diffusion coefficients have been fixed at the value obtained from the DLS experiments performed at identical conditions (solvent, temperature, and extrusion protocol; data from Table I). It is worthy to mention that a good description of the data is reached just with only two adjustable parameters. As mentioned above, this combination of NSE data with DLS experiments has been already applied to successfully analyze the dynamics of microemulsion systems [6,7]. However, a model based in a pure exponential decay for the shape fluctuations [as predicted by the MS theory; Eq. (2)] is absolutely unable to fit the present experimental data, even when the terminal translational term is accounted for. The relative amplitude of the bending mode is obtained near, $1-A\approx0.5$, independently of the wave vector at the studied q range (see the inset in Fig. 7), which assigns the bending mode an important contribution to the observed relaxation.

The relaxation rates of the fluctuation mode seen in the NSE relaxation functions have been plotted in Fig. 7(b). Data are well represented by $\Gamma\sim q^3$ power law, as expected for bending modes. Because the present system can be reasonably rationalized in view of the ZG theory, κ can be easily calculated from the slope of the $\Gamma-q^3$ plot [see Eqs. (13) and (18)]. A value $\kappa=(19\pm2)$ k_BT is obtained for the studied POPC vesicles at 22 °C, in excellent quantitative agreement with values reported by Rawicz *et al.* [44] from micropipette experiments in GUVs and more recently by Kucerka *et al.* [45] from x-ray synchrotron experiments in lamellar phases. However, unphysical values of κ ($\approx0.01k_BT$) are obtained if the MS relation [Eq. (6)] is alternatively used to compute κ from the NSE relaxation rates. Consequently, the present NSE data confirm the ZG theory as the adequate approach to describe relaxation due to bending modes in rigid membranes. In Fig. 8, we discuss again the internal relaxation inferred from DLS autocorrelation functions [see Fig. 5(a)], now in terms of the ZG theory.

The remaining relaxation once isolated by extracting the pure-translation component shows an exponential-like decay

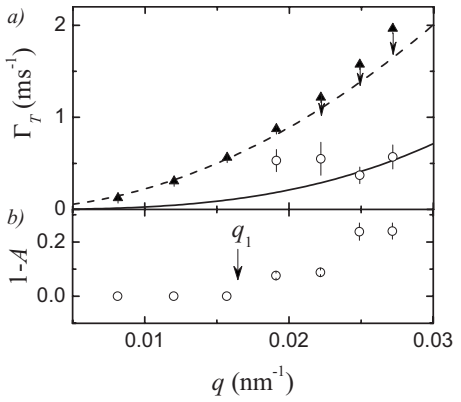

FIG. 9. (a) Results from the reanalysis in Fig. 8. The CONTIN relaxation frequencies of the translational component (triangles) have been shifted to their bare values calculated as $\Gamma_T = D_0 q^2$ (dashed line); then, the internal relaxation is isolated and its relaxation frequency (circles) calculated from the fit to the ZG stretched-exponential decay (see Fig. 8). The solid line represents the theoretical ZG prediction computed for $\kappa = 20 k_B T$ [see Eq. (13)]. (b) Relative amplitudes of the bending mode, as obtained from fittings to the ZG model.

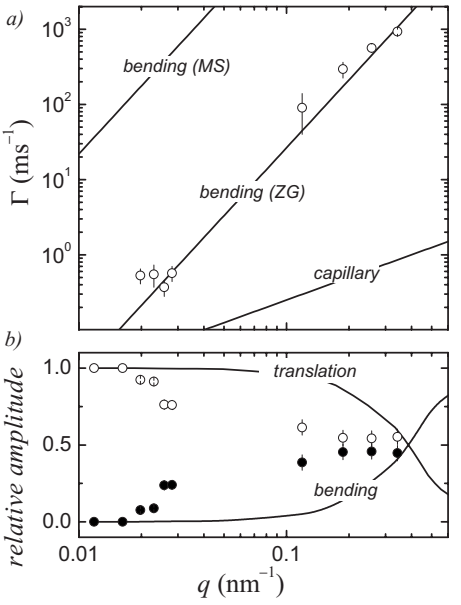

FIG. 10. Dispersion diagram for POPC membranes with bending stiffness $\kappa = 20 k_B T$ and lateral tension $\sigma = 10^{-7}$ N/m: (a) relaxation rates; (b) relative amplitudes (see text for details).

with a terminal tail (not resolvable) eventually entering the time domain corresponding to translation (see Fig. 8). From the above discussion, the pure exponential relaxation arising from MS theory assigns to this relaxation a fast decay (Fig. 8; solid line) with a relaxation rate compatible with a very low unphysical value of κ ($\approx 0.01 k_B T$). However, a reanalysis in terms of the stretched-exponential decay ($\alpha = 2/3$) predicted by ZG (Fig. 8; dashed line) is also able to fit the short-time observable part of the relaxation. However, because of stretching, this relaxation penetrates longer time domains, typically matching the translation time scale. For the sake of example, this analysis is shown in Fig. 8 just at the highest wave vector probed in the DLS regime ($q = 0.027$ nm^{-1}, $l \approx 2$); however, similar fits are possible for every relaxation function plotted in Fig. 5(a). The fitted values of the stretched relaxation rates $\Gamma_f^{(ZG)}$ have been plotted in Fig. 9 as a function of the wave vector.

Although no q dependence is observed within the experimental uncertainty, the absolute values of the experimental relaxation rates $\Gamma_f^{(ZG)}$ are quantitatively compatible with predictions from the ZG theory [see Eq. (13)] calculated for the literature value of $\kappa = 20 k_B T$. This analysis confirms again the suitability of the ZG theory in describing relaxation of the bending modes in rigid vesicles, contrarily to the ground MS theory, which does not account for the dissipation frustration mechanism considered by ZG. In effect, single-exponential relaxation, as predicted by MS, accounts for fast dissipation by bulk friction, however, rigid weakly undulating membranes as those made of lipids are rather inefficient in dissipating elastic energy by viscous friction; thus relaxation is delayed in time resulting in the dissipation mechanism described by ZG and described by a stretched-exponential relaxation at much longer times. As refers to relaxation amplitudes [see Fig. 9(b)], the small relaxation process observed within the DLS scattering, which emerge only at $q \geq q_2$ ($\approx 1/R$), is found increasingly dominant with respect to translation, as expected. Unfortunately, the ZG theory, in its present form, does not supply a precise prediction for the relative amplitude of the fluctuation mode.

Finally, the results obtained corresponding to fluctuation modes are discussed in Fig. 10 together within the frame of the dispersion plot expected from the dynamical theories. At low q's (DLS), we found a relaxation assigned to the first spherical harmonics of the undulation modes ($l \approx 2$). Complementarily, NSE has provided clear evidences on the existence of dominant undulation modes at high q's (corresponding to high harmonics, $l \geq 10$, for which the membrane is essentially seen as a nontranslating near flat entity).

Figure 10(a) shows clearly that the observed relaxation rates obtained as stretched-exponential decays are absolutely compatible with the q^3 dispersion expected from the ZG theory for the relaxation of curvature modes of rigid membranes but completely different to predictions from the MS theory (MS predicts a much faster relaxation than observed). However, before definitely assigning the observed relaxation to bending modes, the present results must be compared with the relaxation characteristics expected for capillary ones. These modes are an alternative class of curvature motion for a membrane, maybe facilitated in rigid membranes where bending is rather costly. Capillary modes are governed by surface-tension forces and could eventually dominate curvature motions at low wave vectors, where undulations create large area excess. However, symmetric lipid bilayers, as the one considered here, are characterized by very low values of surface tension ($\sigma \approx 10^{-7} - 10^{-8}$ N/m); thus surface-tension modes are expected to be marginal and of course relaxing at very slow rates. For overdamped capillary modes, the relaxation rate should be $\Gamma_{cap} = (\sigma / 4\eta) q$, which predicts a weaker dispersion ($\sim q^1$) than bending modes ($\sim q^3$). We have included in Fig. 10(a) predictions from capillary modes, which might be found meaningfully slower than the relaxation

modes experimentally observed. Furthermore, the observed relaxation is clearly compatible with a q^3-dispersive behavior typical of bending modes but not of capillary ones. Therefore, we deduce that the observed bending modes relax in a way compatible with predictions from ZG theory. Figure 10(b) shows the q dependence of the mode amplitudes. As expected, the bending mode contributes more and more to relaxation as q increases, becoming dominant at a crossover regime just at the onset of the NSE window ($q \geq 0.1$ nm^{-1}), in rough qualitative agreement with the theoretical amplitudes [as calculated from Eq. (A5)]. We can conclude therefore that the ZG theory represents the adequate frame for explaining relaxation of bending modes in rigid bilayers, where curvature modes are inefficient in exploring the bulk for adequate dissipation. Though the MS theory captures the essential dynamical features, it fails in describing relaxation over short times and small distances with respect to the fundamental relaxation process captured at the hydrodynamic core of the MS theory. The main concept that emerged from the ZG formalism is that rigid membranes frustrate regular dissipation at the subrelaxation dynamical regime [$t < 4\eta/\kappa q^3, q > (4\eta/\kappa t)^{1/3}$], resulting in an effective relaxation as a stretched-exponential decay. Floppy surfaces, such as microemulsion droplets fluctuating at the lowest modes, dissipate however regularly, resulting in the single-exponential relaxation experimentally observed. The ZG theory appears therefore as the dynamical extension of MS concepts necessary for describing fluctuation dynamics of rigid vesicles in suspension.

V. CONCLUSIONS

We have experimentally probed the relaxation of bending fluctuation modes of rigid lipid (POPC) vesicles in diluted suspensions. The combined analysis of DLS and NSE data has allowed for discriminating the two relaxation modes expected: Brownian translation of the vesicle as a whole (with diffusion coefficient governed by Stokes friction) and curvature fluctuations. The relaxation rates of the curvature fluctuations are found to follow a dispersion $\Gamma_f \sim q^3$ characteristic of bending modes of an elastic membrane dissipating against the bulk phase by viscous friction. The quantitative analysis of the absolute values of Γ_f and of the relative bending fluctuation amplitudes in view of the MS theory of spherical droplets and vesicles assigns a fluctuation dynamics typical for a very floppy membrane ($\kappa_{MS} < k_B T$), in complete incongruity with the rigid character of lipid bilayer membranes ($\kappa \gg k_B T$). Furthermore, the observed relaxation functions are found compatible with a stretched-exponential decay with a much slower relaxation rate than expected from the usual dissipation mechanism $\Gamma_f = (\kappa/4\eta)q^3$, which assigns relaxation of a rigid membrane occurring at a much higher effective viscosity and/or through of a frustrated dissipation mechanism, which takes longer times to relax curvature fluctuations by bulk friction. The Zilman-Granek extension of the MS theory has been invoked to account for these discrepancies between theory and experiment. Compared to the floppy character of microemulsion droplets, where the MS theory has been extensively found successfully in describing fluctuation dynamics, the much weaker fluctuations of rigid vesicles based on lipid bilayers accomplish the physical terms considered by the ZG theory to bring in a frustrated dissipation mechanism characterized by a stretched-exponential relaxation. The analysis of the experimental relaxation data in terms of the ZG theory leads to reliable values of the bending constant ($\kappa_{ZG} \approx 20\ k_B T$ for POPC) in agreement with literature data. From the above results, we state that both theories are complementary in the sense that both describe similar kinds of systems in different dynamic limits or systems completely different defined by extreme values of the bending rigidity. As a final remark, we must state that while the MS theory is closed in the sense that it describes membrane dynamics at the spherical topology, the ZG approach for rigid planar membranes certainly does not solve the equations for vesicles as the MS theory does. Consequently, the theory of vesicle fluctuations might advance in the sense of a rigorous description of the frustrated ZG mechanism in the spherical topology.

ACKNOWLEDGMENTS

This work was supported by Grants No. FIS2006-01305 and No. CSD2007-0010 (Consolider Ingenio en Nanociencia Molecular) from MICINN and Grant No. S-0505/MAT/0283 from CAM (Spain), Grants No. Sfb 448 and No. TP A12 from DFG (Germany) and Marie-Curie-RTN *POLYAMPHI* from European Union. L.R.A. was supported by FPI-CAM and I.L.-M. from NANOBIO-M [49] (Grant No. CAM S-0505/MAT/0283).

APPENDIX: MILNER-SAFRAN THEORY

In the MS model, small quadratic changes in curvature with respect to the equilibrium value $(H-H_S)^2 = 4[(1/R) - (1/R_S)]^2 = (4/R_0^2)[(R_0/R) - (R_0/R_S)]^2 = (4/R_0^2)[(R_0/R) - w]^2$ are expanded up to second in the deformation, i.e., $R_0/R = (1+\delta)^{-1} \approx 1 - \delta + \delta^2$. The dimensionless parameter $w = R_0/R_S$ gives idea form the deviation with respect to the spontaneous curvature ($w=0$ if $H_S=0$). After equipartition, once the constant area and volume constraints are imposed, thermal fluctuations are found with mean-square amplitudes,

$$\langle u_{lm}^2 \rangle = \frac{k_B T}{\kappa} \frac{1}{(l+2)(l-1)[l(l+1) - 4w + 2w^2]}. \quad \text{(A1)}$$

At low Reynolds numbers, the hydrodynamic motion is governed by Stokes flow. When inertial and convective terms are neglected in the Navier-Stokes equation, the dynamical fluctuations are obtained as exponential solutions, i.e., $u(t) = \Sigma_{l,m} u_{lm} Y_{lm} \exp(\Gamma_l t)$. It is important to notice that Eq. (A1) is only valid for undulation modes $l \geq 2$ since $l=1$ corresponds to the translation displacement of the droplet as a whole requiring no bending energy. This mode ($l=1$) is essentially related to the Brownian motion of the droplet. The MS model discusses the deterministic solutions in view of fluctuation-dissipation theorem to obtain autocorrelation functions for the thermal undulations,

$$\langle u_{lm}(t)u_{lm}^*(0)\rangle = \langle u_{lm}^2\rangle \exp(-\Gamma_l t), \tag{A2}$$

where the amplitude of the quadratic fluctuations of the l mode is given by Eq. (A1) and its relaxation rate Γ_l,

$$\Gamma_l = \frac{\kappa}{\eta R_0^3}\frac{l(l+1)-4w+2w^2}{Z(l)}, \tag{A3}$$

where η is the viscosity of the bulk fluid; the l-dependent Z factor is given by

$$Z(l) = \frac{(2l+1)(2l^2+2l-1)}{l(l+1)(l+2)(l-1)}. \tag{A4}$$

Following the general formalism for quasielastic scattering [29,50], MS compute the dynamic structure factor from a shell-like object as

$$S(q,t) \approx \exp(-D_T q^2 t)\left[4\pi j_0^2(qR_0) + \sum_{l\geq 2} F_l(qR_0)\langle u_{l0}(t)u_{l0}^*(0)\rangle\right], \tag{A5}$$

where the weighting factor $F_l(qR_0)$ is defined as

$$F_l(z) = (2l+1)[(l+2)j_l(z) - zj_{l+1}(z)]^2 \tag{A6}$$

and $j_l(z)$ are the spherical Bessel functions on the order of l.

The relationship in Eq. (A5) states that the vesicle diffuses as a whole at a rate $\Gamma_T = D_T q^2$, which is governed by the Stokes-Einstein diffusion coefficient,

$$D_T = \frac{k_B T}{6\pi\eta R_0}. \tag{A7}$$

The series of fluctuation modes in Eq. (A5) appears subordinated to the translational term, which establishes that the relaxation of every undulation mode is individually affected by translation. The two terms in Eq. (A5) weakly oscillate, the pure-translational term ($\sim j_0^2$) being progressively decreasing with qR_0, while the sum corresponding to the undulation modes ($\sim \Sigma_l F_l$) becomes conversely dominant at high q (see Fig. 1 in main text).

[1] W. Helfrich, Z. Naturforsch. C **28**, 693 (1973).
[2] S. T. Milner and S. A. Safran, Phys. Rev. A **36**, 4371 (1987).
[3] J. T. Jenkins, J. Math. Biol. **4**, 149 (1977).
[4] M. B. Schneider, J. T. Jenkins, and W. W. Webb, J. Phys. (Paris) **45**, 1457 (1984).
[5] J. S. Huang, S. T. Milner, B. Farago, and D. Richter, Phys. Rev. Lett. **59**, 2600 (1987).
[6] T. Hellweg and D. Langevin, Phys. Rev. E **57**, 6825 (1998).
[7] T. Hellweg, A. Brûlet, and T. Sottmann, Phys. Chem. Chem. Phys. **2**, 5168 (2000).
[8] J. Pécréaux, H.-G. Döbereiner, J. Prost, J.-F. Joanny, and P. Bassereau, Eur. Phys. J. E **13**, 277 (2004).
[9] E. Evans and W. Rawicz, Phys. Rev. Lett. **79**, 2379 (1997).
[10] R. Rodríguez-García, L. R. Arriaga, M. Mell, L. H. Moleiro, I. López-Montero, and F. Monroy, Phys. Rev. Lett. **102**, 128101 (2009).
[11] L. R. Arriaga, I. López-Montero, F. Monroy, G. Orts-Gil, B. Farago, and T. Hellweg, Biophys. J. **96**, 3629 (2009).
[12] W. Li and T. H. Haines, Biochemistry **25**, 7477 (1986).
[13] T. H. Haines, W. Li, M. Green, and H. Z. Cummins, Biochemistry **26**, 5439 (1987).
[14] P. Brocca, L. Cantù, M. Corti, and E. D. Favero, Prog. Colloid Polym. Sci. **115**, 181 (2000).
[15] P. Brocca, L. Cantù, M. Corti, E. D. Favero, and S. Motta, Langmuir **20**, 2141 (2004).
[16] *Mechanics of the Cell*, edited by D. Boal (Cambridge University Press, Cambridge, 2002).
[17] R. Messager, P. Bassereau, and G. Porte, J. Phys. (Paris) **51**, 1329 (1990).
[18] F. Brochard and J.-F. Lennon, J. Phys. (Paris) **36**, 1035 (1975).
[19] E. Freyssingeas, D. Roux, and F. Nallet, J. Phys.: Condens. Matter **8**, 2801 (1996).
[20] E. Freyssingeas, F. Nallet, and D. Roux, Langmuir **12**, 6028 (1996).
[21] A. G. Zilman and R. Granek, Phys. Rev. Lett. **77**, 4788 (1996).
[22] A. G. Zilman and R. Granek, Chem. Phys. **284**, 195 (2002).
[23] S. A. Safran, Phys. Rev. A **43**, 2903 (1991).
[24] D. J. Mitchell and B. W. Ninham, J. Chem. Soc., Faraday Trans. 2 **77**, 601 (1981).
[25] P. G. De Gennes and C. Taupin, J. Phys. Chem. **86**, 2294 (1982).
[26] H. T. Jung, S. Y. Lee, E. W. Kaler, B. Coldren, and J. A. Zasadzinski, Proc. Natl. Acad. Sci. U.S.A. **99**, 15318 (2002).
[27] S. A. Safran, J. Chem. Phys. **78**, 2073 (1983).
[28] G. Brannigan and F. L. H. Browny, Biophys. J. **92**, 864 (2007).
[29] B. J. Berne and R. Pecora, *Dynamic Light Scattering* (Wiley, New York, 1976).
[30] B. Farago, D. Richter, J. S. Huang, S. A. Safran, and S. T. Milner, Phys. Rev. Lett. **65**, 3348 (1990).
[31] B. Farago, M. Monkenbusch, K. D. Goecking, D. Richter, and J. S. Huang, Physica B **213-214**, 712 (1995).
[32] B. Farago and M. Gradzielski, J. Chem. Phys. **114**, 10105 (2001).
[33] For small deformations, $u_q \sim u_0 e^{iqr}$, the changes in local curvature are approximated by $\delta H \approx \nabla^2 u_q$, thus, the energy cost in creating a bending deformation with wave vector q is $\delta F_q \sim 1/2\kappa(\nabla^2 u_q)^2 \sim 1/2\kappa q^4 u_q^2$; consequently, for thermal modes, $\langle u_q^2\rangle \sim k_B T/\kappa q^4$.
[34] C. R. Safinya, D. Roux, G. S. Smith, S. K. Sinha, P. Dimon, N. A. Clark, and A. M. Bellocq, Phys. Rev. Lett. **57**, 2718 (1986).
[35] S. S. Sorlie and R. Pecora, Macromolecules **23**, 487 (1990).
[36] S. S. Sorlie and R. Pecora, Macromolecules **21**, 1437 (1988).
[37] R. Granek, J. Phys. II **7**, 1761 (1997).

[38] J. Beaucourt, F. Rioual, T. Séon, T. Biben, and C. Misbah, Phys. Rev. E **69**, 011906 (2004).
[39] N. Shahidzadeh, D. Bonn, O. Aguerre-Chariol, and J. Meunier, Phys. Rev. Lett. **81**, 4268 (1998).
[40] S. W. Provencher, Comput. Phys. Commun. **27**, 213 (1982).
[41] S. W. Provencher, Comput. Phys. Commun. **27**, 229 (1982).
[42] A. Jakes, Collect. Czech. Chem. Commun. **60**, 1781 (1995).
[43] P. Schleger *et al.*, Physica B **266**, 49 (1999).
[44] W. Rawicz, K. C. Olbrich, T. McIntosh, D. Needham, and E. Evans, Biophys. J. **79**, 328 (2000).
[45] N. Kucerka, S. Tristram-Nagle, and J. F. Nagle, J. Membr. Biol. **208**, 193 (2005).
[46] P. J. Patty and B. Frisken, Appl. Opt. **45**, 2209 (2006).
[47] J. Evans, W. Gratzer, N. Mohandas, K. Parker, and J. Sleep, Biophys. J. **94**, 4134 (2008).
[48] D. E. Discher and F. Ahmed, Annu. Rev. Biomed. Eng. **8**, 323 (2006).
[49] www.nanobiom.org.
[50] S. W. Lovesey and P. Schofield, J. Phys. C **9**, 2843 (1976).